Square deployable frames for space applications. Part 2: realization

Y Chen[1] and **Z You**[2]*
[1]School of Mechanical and Aerospace Engineering, Nanyang Technological University, Singapore, Singapore
[2]Department of Engineering Science, University of Oxford, Oxford, UK

The manuscript was received on 15 March 2006 and was accepted after revision for publication on 23 August 2006.

DOI: 10.1243/09544100JAERO100

Abstract: In a sister paper, the authors have proved mathematically that the three-dimensional 4*R* overconstrained Bennett linkage has an alternative form allowing it to be folded up completely. In this paper, the ways of building such structures are shown. For design purposes, a set of design parameters is introduced that could be used for rapid prototyping because they are closely linked with the final expanded configuration. The relationships between the design and geometrical parameters, commonly used to describe the Bennett linkages by kinematicians, have been derived. Moreover, the concept of a single compact folding Bennett linkage has been extended to a grid in which the Bennett linkages are nested within each other. The new assembly retains all the common features of the single linkage. A series of physical models were made, which successfully demonstrate the concept.

Keywords: deployable structure, Bennett linkage, bar assembly, alternative form, grid of linkages

1 INTRODUCTION

The Bennett linkage is a three-dimensional overconstrained mechanism consisting of four bars connected by revolute hinges. In the preceding paper [**1**], a concept based on the alternative forms of the linkage has been presented, which allows compact folding and maximum expansion of the linkage. Like much research on the theory of mechanisms, our analysis did not consider the geometrical dimension of the members forming the linkage. However, to construct a physical model, it is necessary to use members and joints whose sizes are finite and cannot be simply neglected.

According to Crawford *et al.* [**2**], for a closed loop consisting of n bars with identical cross-section, the cross-section of the whole structure in the folded configuration should be a regular n-gon in order to achieve the most compact folding. Applying this principle to the alternative form of the Bennett linkage, each link should be made of bars with square cross-section. Pellegrino *et al.* [**3**] revealed a model of a 4*R* linkage, which is, in fact, an alternative form of the Bennett linkage. Figure 1 shows such a model, although angle ω in the reported model was $\pi/4$ in the fully deployed configuration. This particular example shows that construction of a Bennett linkage with compact folding and maximum expansion is not only mathematically feasible, as proved in the preceding paper, but also practically possible.

For convenience, the model shown in Fig. 1 is used to define the key design parameters. The model consists of four bars with square cross-section. When it is fully packaged, it forms a square in which each quarter corresponds with the section of one of the bars. The three design parameters are L and ω, denoted as the bar length in the alternative form of the linkage and half of one of the angles between two adjacent bars, respectively, and λ, as the tilted angle of the square section with respect to the plane on which the linkage in its alternative form lies. The other angle between two adjacent bars in the alternative form is $2(\pi/2 - \omega)$. The number of design parameters matches with that presented in the preceding paper in which the geometrical parameters are l, α, c (or d), which are more useful

*Corresponding author: Department of Engineering Science, University of Oxford, Parks Road, Oxford OX1 3PJ, UK. email: zhong.you@eng.ox.ac.uk

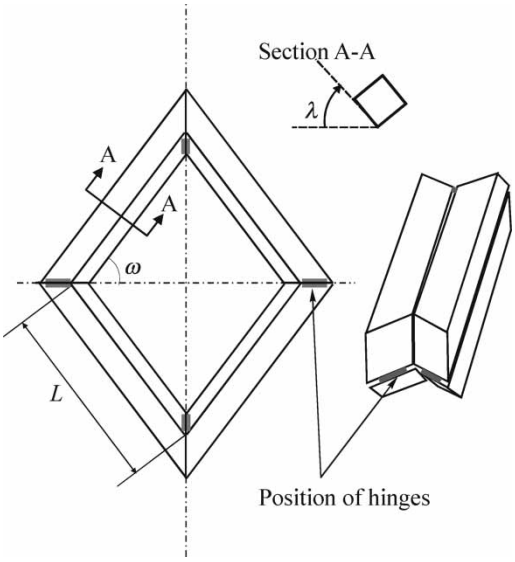

Fig. 1 The alternative form of the Bennett linkage made from square cross-section bars in the deployed and folded configurations

in the geometrical analysis and make the derivations simpler. In next section, the relationships between two sets of parameters are established.

2 GEOMETRICAL RELATIONSHIPS OF DESIGN PARAMETERS

2.1 Parameters λ and ω

Figure 2 shows a fully deployed linkage EFGH, which is the alternative form of the Bennett linkage. The linkage has reached its maximum expansion, thus EFGH becomes a planar rhombus. For ease of description, a Cartesian coordinate system is defined where axes x and y are collinear with FH and EG, respectively. The linkage EFGH is, therefore, symmetric about both xoz and yoz planes where o is the centre of EFGH and axis z is normal to plane xoy. Now introduce a square bar, shown in grey colour in Fig. 2, as link FG in such a way that one of the edges of the square bar lies along FG. The bar is terminated by planes GIJK and FUVW, created by slicing the bar with the planes yoz and xoz, respectively. Obviously, the axes of the revolute joints at two ends of the bar should be GI and FU because they are part of lines GP and FQ, respectively.

An enlarged diagram of bar FG is shown in Fig. 3(a). A plane x′o′y′ that is just in touch with the bar at J and V and parallel to plane xoy is defined. A typical square cross-section of the bar is marked as RXYZ. The projection of the bar is given in Fig. 3(b), in which X′, R′, and Z′, etc. represent the projection of X, R, Z, etc. on the plane x′o′y′.

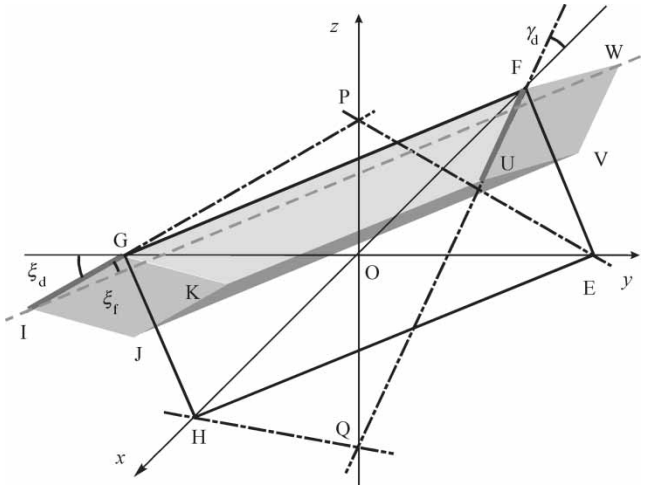

Fig. 2 The alternative form of the Bennett linkage with square cross-section bars in the deployed configuration

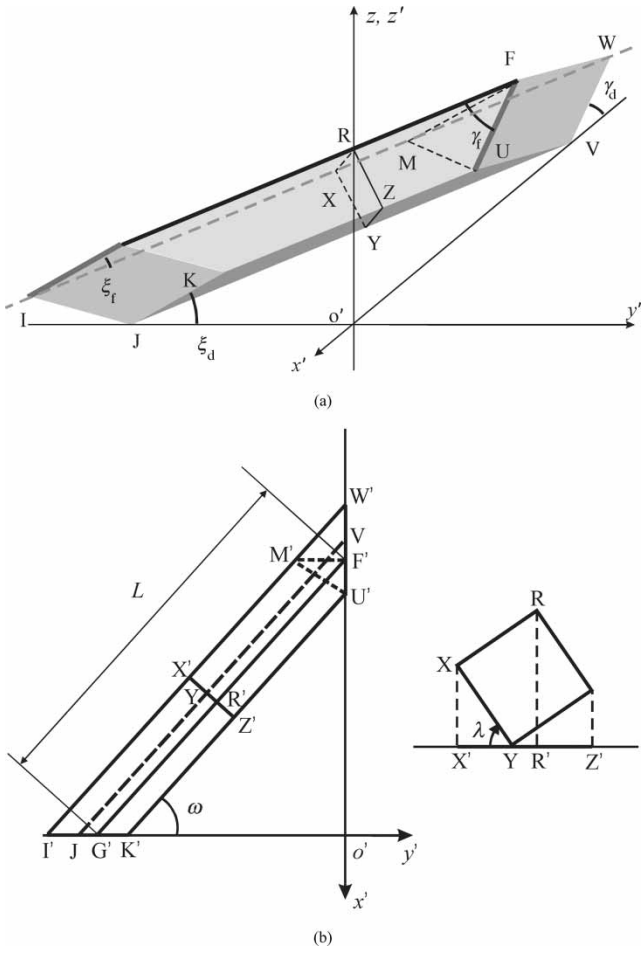

Fig. 3 The geometry of the square cross-section bar: (a) in three-dimension and (b) projection on the plane x′o′y′ and the enlarged cross-section RXYZ

Assume

$$\overline{RX} = \overline{XY} = \overline{YZ} = \overline{ZR} = 1$$

The following relationships can be obtained from Fig. 3(b)

$$\overline{X'Y} = \overline{R'Z'} = 1 \cdot \cos\lambda$$
$$\overline{X'R'} = \overline{Y'Z'} = 1 \cdot \sin\lambda$$
$$\overline{X'Z'} = 1 \cdot (\sin\lambda + \cos\lambda)$$
$$\overline{II'} = \overline{XX'} = \overline{WW'} = 1 \cdot \sin\lambda$$
$$\overline{KK'} = \overline{ZZ'} = \overline{UU'} = 1 \cdot \cos\lambda$$
$$\overline{F'U'} = \overline{VW'} = \frac{\overline{R'Z'}}{\cos\omega} = \frac{\cos\lambda}{\cos\omega}$$
$$\overline{F'W'} = \overline{U'V} = \frac{\overline{X'R'}}{\cos\omega} = \frac{\sin\lambda}{\cos\omega}$$
$$\overline{G'K'} = \overline{I'J} = \frac{\overline{R'Z'}}{\sin\omega} = \frac{\cos\lambda}{\sin\omega}$$

and

$$\overline{G'I'} = \overline{JK'} = \frac{\overline{X'R'}}{\sin\omega} = \frac{\sin\lambda}{\sin\omega}$$

thus

$$\overline{GI} = \overline{JK} = \sqrt{\overline{JK'}^2 + \overline{KK'}^2} = \sqrt{\frac{\sin^2\lambda}{\sin^2\omega} + \cos^2\lambda} \tag{1}$$

and

$$\overline{FU} = \overline{VW} = \sqrt{\overline{VW'}^2 + \overline{WW'}^2}$$
$$= \sqrt{\frac{\cos^2\lambda}{\cos^2\omega} + \sin^2\lambda} \tag{2}$$

Now in Fig. 3(a), line FM is drawn which is parallel to GI and crosses IW at M. Thus, $\angle$MFU is the angle between two axes of the adjacent joints, that is

$$\angle MFU = \alpha$$

and

$$\cos\alpha = \frac{\overline{FM}^2 + \overline{FU}^2 - \overline{UM}^2}{2 \cdot \overline{FM} \cdot \overline{FU}} \tag{3}$$

Because FM is parallel to GI and FG to MI

$$\overline{FM} = \overline{GI} = \sqrt{\frac{\sin^2\lambda}{\sin^2\omega} + \cos^2\lambda} \tag{4}$$

and

$$\overline{F'M'} = \overline{G'I'} = \frac{\sin\lambda}{\sin\omega} \tag{5}$$

Since F′M′ is perpendicular to W′U′

$$\overline{U'M'}^2 = \overline{F'M'}^2 + \overline{F'U'}^2 \tag{6}$$

Moreover

$$\overline{UM}^2 = \overline{U'M'}^2 + (\overline{MM'} - \overline{UU'})^2 \tag{7}$$

Substituting equations (2), (4), and (7) into equation (3) gives

$$\cos\alpha = \pm \frac{\sin 2\lambda \sin 2\omega}{\sqrt{\sin^2 2\lambda \sin^2 2\omega + 8(1 - \cos 2\lambda \cos 2\omega)}} \tag{8}$$

Equation (8) is the relationship between design parameters ω and λ for a given twist α of the original Bennett linkage, which is plotted in Fig. 4. It is interesting to note that for $0 \leqslant \lambda \leqslant \pi/2$ and $0 \leqslant \omega \leqslant \pi/2$, the range of α is between $\arccos(1/3)$ and $\pi - \arccos(1/3)$, which is the same as that obtained from equation (29) in the preceding paper.

The precise values for ω and λ in a physical model are determined by θ_d, φ_d, θ_f, and φ_f, which are the revolute variables in association with the folded and deployed configurations of the linkage. This relationship is described later.

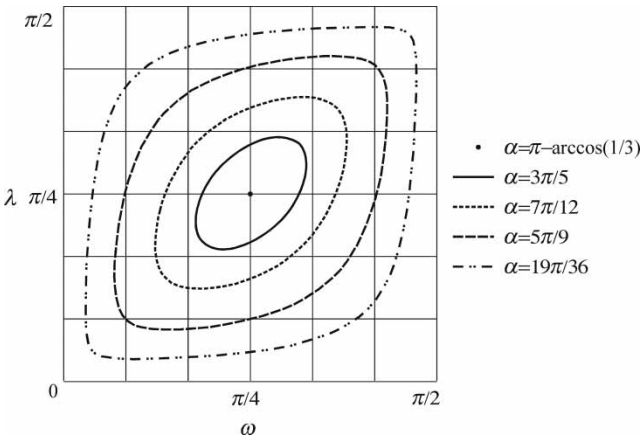

Fig. 4 λ versus ω for a set of given α

As described in equation (15) of the preceding paper, in the deployed configuration

$$\cos\angle\mathrm{EPG} = 2\frac{1+\cos\varphi_\mathrm{d}}{1-\cos\theta_\mathrm{d}} - 1 \quad \text{and}$$
$$\cos\angle\mathrm{FQH} = 2\frac{1+\cos\theta_\mathrm{d}}{1-\cos\varphi_\mathrm{d}} - 1 \tag{9}$$

From Fig. 2

$$\angle\mathrm{EPG} = \pi - 2\xi_\mathrm{d} \quad \text{and} \quad \angle\mathrm{FQH} = \pi - 2\gamma_\mathrm{d} \tag{10}$$

From Fig. 3(a)

$$\tan\xi_\mathrm{d} = \frac{\overline{\mathrm{KK'}}}{\overline{\mathrm{JK'}}} = \frac{\cos\lambda}{\sin\lambda/\sin\omega} \quad \text{and}$$
$$\tan\gamma_\mathrm{d} = \frac{\overline{\mathrm{WW'}}}{\overline{\mathrm{VW'}}} = \frac{\sin\lambda}{\cos\lambda/\cos\omega} \tag{11}$$

Substituting equation (10) into equation (9) and then considering equation (11), the following equations are obtained

$$\cos\theta_\mathrm{d} = \frac{(\cos 4\lambda - 1) + (\cos 4\lambda\cos 2\omega - 4\cos 2\lambda + 3\cos 2\omega)}{4(1-\cos 2\omega\cos 2\lambda)} \tag{12a}$$

and

$$\cos\varphi_\mathrm{d} = \frac{(\cos 4\lambda - 1) - (\cos 4\lambda\cos 2\omega - 4\cos 2\lambda + 3\cos 2\omega)}{4(1-\cos 2\omega\cos 2\lambda)} \tag{12b}$$

When the linkage is folded up, EFGH becomes a bundle ST, so do all of the bars with square cross-section. Bar EF in this particular configuration is shown in Fig. 5.

Similar to equation (9), in the folded configuration

$$\cos\angle\mathrm{ATC} = 2\frac{1+\cos\varphi_\mathrm{f}}{1-\cos\theta_\mathrm{f}} - 1 \quad \text{and}$$
$$\cos\angle\mathrm{BSD} = 2\frac{1+\cos\theta_\mathrm{f}}{1-\cos\varphi_\mathrm{f}} - 1 \tag{13}$$

From Fig. 5

$$\angle\mathrm{ATC} = 2\xi_\mathrm{f} \quad \text{and} \quad \angle\mathrm{BSD} = 2\gamma_\mathrm{f} \tag{14}$$

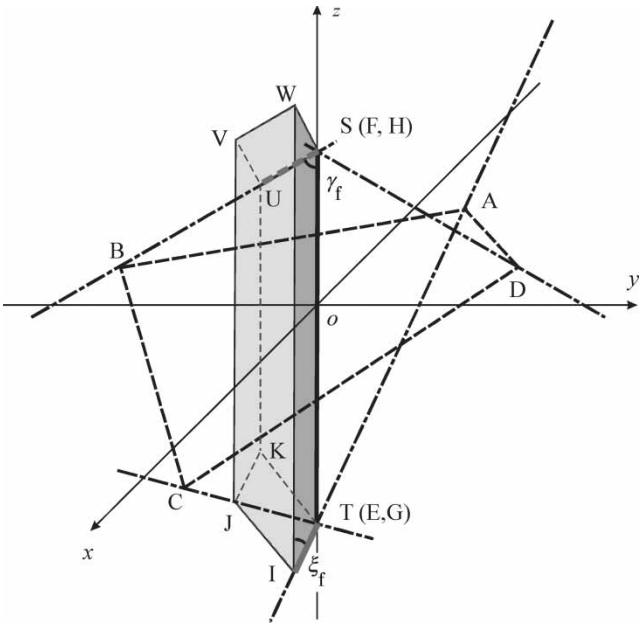

Fig. 5 The alternative form of the Bennett linkage with square cross-section bars in the folded configuration

From Fig. 2

$$\tan\xi_\mathrm{f} = \frac{\overline{\mathrm{RX}}}{\overline{\mathrm{XI}} - \overline{\mathrm{RG}}} = \frac{\overline{\mathrm{RX}}}{\overline{\mathrm{R'X'}}/\tan\omega} = \frac{\tan\omega}{\sin\lambda} \quad \text{and} \quad \tan\gamma_\mathrm{f} = \frac{\overline{\mathrm{RZ}}}{\overline{\mathrm{RF}} - \overline{\mathrm{UZ}}} = \frac{\overline{\mathrm{RZ}}}{\overline{\mathrm{R'Z'}}\tan\omega} = \frac{1}{\cos\lambda\tan\omega} \tag{15}$$

Now substituting equation (14) into equation (13) and then considering equation (15), the following relationships are obtained

$$\cos\theta_\mathrm{f} = \frac{(\cos 4\omega - 1) + (\cos 4\omega\cos 2\lambda - 4\cos 2\omega + 3\cos 2\lambda)}{4(1-\cos 2\omega\cos 2\lambda)} \tag{16a}$$

and

$$\cos\varphi_\mathrm{f} = \frac{(\cos 4\omega - 1) - (\cos 4\omega\cos 2\lambda - 4\cos 2\omega + 3\cos 2\lambda)}{4(1-\cos 2\omega\cos 2\lambda)} \tag{16b}$$

Note that θ_d and φ_d as well as θ_f and φ_f are coupled because

$$\tan\frac{\theta}{2}\tan\frac{\varphi}{2} = \frac{1}{\cos\alpha}$$

so using one equation each from equation (12) and (16), λ and ω can be solved if the values of θ_d (or φ_d) and θ_f (or φ_f) are given.

2.2 Parameter *L*

L is the actual side length of the alternative form of the Bennett linkage. In the preceding paper, it was shown that

$$\frac{L}{l} = \sqrt{-\frac{2}{\cos\theta_{\mathrm{f}} + \cos\varphi_{\mathrm{f}}}}$$

which is equation (31) in [**1**]. Substituting equation (16) into the above equation yields

$$\frac{L}{l} = 2\sqrt{\frac{1 - \cos 2\omega \cos 2\lambda}{1 - \cos 4\omega}} \tag{17}$$

When the deployed configuration of the alternative form is a square, that is $\omega = \pi/4$, equation (17) gives

$$\frac{L}{l} = \sqrt{2}$$

In the preceding paper, it was shown that both c and d can be written as

$$c = -l\sqrt{\frac{(1 + \cos\varphi_{\mathrm{f}})(1 - \cos\theta_{\mathrm{f}})}{-2(\cos\varphi_{\mathrm{f}} + \cos\theta_{\mathrm{f}})}} \quad \text{and}$$

$$d = -l\sqrt{\frac{(1 - \cos\varphi_{\mathrm{f}})(1 + \cos\theta_{\mathrm{f}})}{-2(\cos\varphi_{\mathrm{f}} + \cos\theta_{\mathrm{f}})}}$$

which is equation (21) in [**1**]. Hence, the following relationships can be obtained noting equation (17)

$$\frac{c}{l} = \frac{\cos\lambda \sin^2\omega}{\cos\omega}\sqrt{\frac{1 - \sin^2\omega \sin^2\lambda}{\sin^2\lambda \cos^2\omega + \sin^2\omega \cos^2\lambda}}$$

and

$$\frac{d}{l} = \frac{\sin\lambda \cos^2\omega}{\sin\omega}\sqrt{\frac{1 - \cos^2\omega \cos^2\lambda}{\sin^2\lambda \cos^2\omega + \sin^2\omega \cos^2\lambda}} \tag{18}$$

Table 1 Key design and geometrical parameters for the models

	λ (rad)	ω (rad)	α (rad)	c/l	d/l
Model 1 (Fig. 6)	$\pi/4$	$\pi/4$	1.9106	0.6124	0.6124
Model 2 (Fig. 7)	$\pi/6$	$53\pi/180$	1.84	1.1156	0.2566
Model 3 (Fig. 8)	$\pi/4$	$\pi/3$	1.8679	1.1858	0.27

So far, a set of equations has been obtained relating geometrical parameters of an alternative form of the Bennett linkage to the design parameters, based on which a model consisting of four square cross-section bars can be built together with hinges on the positions of the axes of the revolute joints, as described in Fig. 1.

In practice, it is not necessary to know the characteristics of the original Bennett linkage l, α, and extended distance on the axes of joints c (or d) unless geometrical analysis needs to be conducted. The design work can be done on the basis of the values of L, λ, and ω, although it is much more convenient to use l, α and c (or d) when analysing the kinematic behaviour of the linkage such as θ_{d}, φ_{d}, θ_{f}, and φ_{f}. Several models have been made using wooden bars of square cross-section and door hinges. The key parameters of these models are given in Table 1 and their expansion sequences are shown in Figs 6 to 8.

3 NETWORK OF THE BENNETT LINKAGES

In the early publications [**4**, **5**], it was shown that a grid-like assembly of Bennett linkages could be made, which retained the single degree of mobility. It was possible to form profiles ranging from helical to planar surfaces. A schematic drawing of a particular grid-like assembly is shown in Fig. 9. The assembly is made from many large and small equilateral Bennett linkages. Each of the straight line in the diagram represents a single bar and the crossing points between these bars are the locations of hinges. The skewed angles between two neighbouring hinges are α and $-\alpha$, which are marked alongside the bars. In the original form of the Bennett linkages,

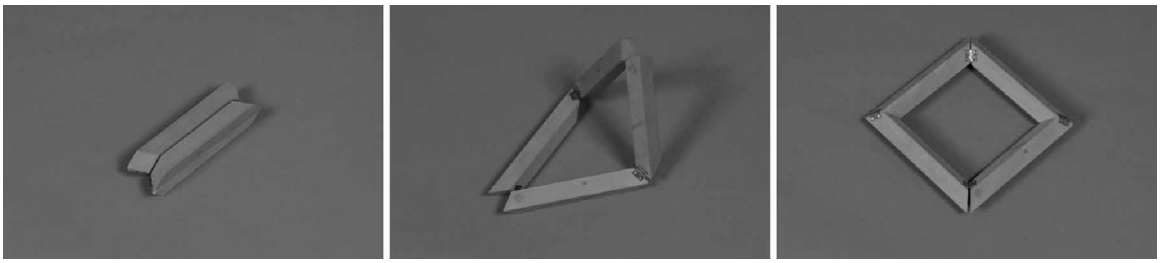

Fig. 6 Expansion sequence of model 1 that opens up to form a square

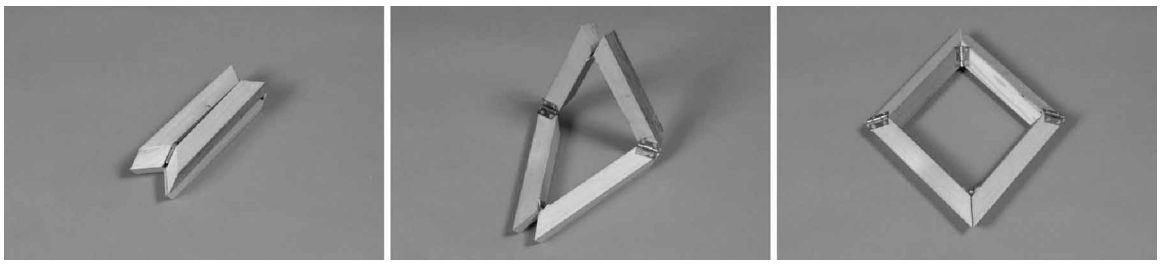

Fig. 7 Expansion sequence of model 2 that opens up to a diamond shape

these bars are the shortest distance between two neighbouring hinges. The expanded grid forms a flat profile. Moreover, it can be extended by repeatedly adding Bennett linkages.

The authors have found that based on this mobile grid, it is also possible to construct a grid-like network of Bennett linkages in their alternative forms that allow compact packaging.

Figure 10(a) illustrates how such an assembly can be built in three-dimension. To avoid overcrowding, only three members, M1, M2, and M3, are shown, which form part of the Bennett linkages B1, B2, and B3. Note that B1 and B3 are the larger Bennett linkages and B2 is the smaller one located at the corners of the larger Bennett linkages (refer to Fig. 9). On the right of the figure is member M1, which is identical to the member shown in Fig. 2 except at both ends. The difference is due to the fact that there are four hinges on each member in a Bennett grid displaced in Fig. 9. Hence, the ends have to be made shorter by slicing off some materials to prevent obstructing deployment. In M1, hinges 1–1 and 2–2 are identical to hinges FU and GI shown in Fig. 2. Hinges 3–3 and 4–4 are newly added. At the left end of M1, hinge 4–4 is used to connect to member M2 in the Bennett linkage B2, whereas hinge 2–2 is used to connect the adjacent member in the Bennett linkage B1, which is not shown in the figure because the connection is the same as in a single Bennett linkage in its alternative form. Member M2 is then connected to another member M3, which is identical to M1, together with the two members absent from the figure forming Bennett linkage B3. The dash–dot lines in Fig. 10(a) show the location of the axes of the hinges.

Figure 10(b) shows the original Bennett linkages corresponding to B1, B2, and B3 shown in Fig. 10(a). The hinge lines are kept for easy comparison with Fig. 10(a). Careful readers may note that B1 and B2 seem not connected. In fact, this is not the case. Take C_1D_1 and C_2D_2 as an example. Because they are parallel and are at a fixed distance away from each other at all the time during the movement of linkages, a rigid link connecting $D_1C_1C_2D_2$ can be built. The same applies to other links also. Hence, the grid in the original form matches with that shown in Fig. 9.

A series of photos in Figs 11(a) to (c) show the deployment sequence of a physical model. It is made of hollow circular tubes with end blocks, which were used to position the hinge axes, and door hinges. Figure 10(d) shows how the hinges are positioned. It deploys smoothly. The behaviour of each Bennett linkage in the assembly is exactly the same as that of a single Bennett linkage in its alternative form.

4 CONCLUSION AND DISCUSSIONS

The preceding paper presented a mathematical proof of the existence of alternative forms of the Bennett linkage, which is capable of achieving compact folding and maximum expansion. In this paper, the authors have made construction of deployable models possible. For design purposes, a set of design parameters is introduced. These parameters could be used for rapid prototyping because they are closely linked with the final expanded

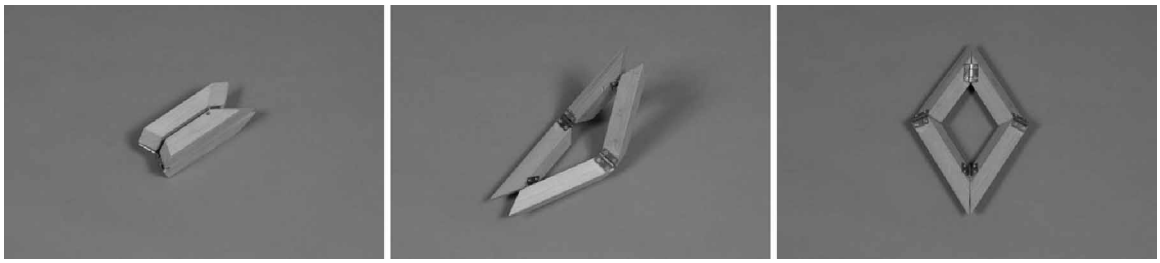

Fig. 8 Expansion sequence of model 3 that opens up to a diamond shape

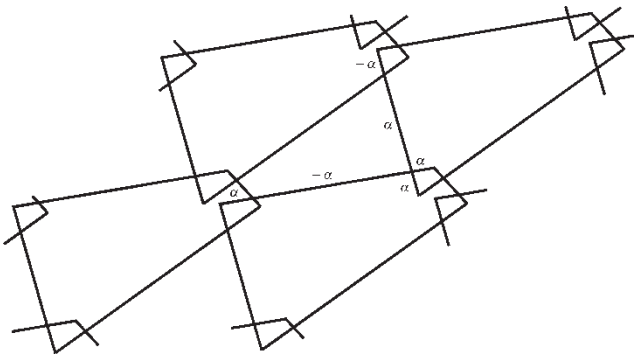

Fig. 9 The schematic diagram of a grid-like assembly of equilateral Bennett linkages

configuration. At the same time, the relationships between the design and geometrical parameters have been established. Therefore, the geometrical parameters can be used for the computation of motion paths. This has been proved to be extremely useful in a similar application that deals with six-bar overconstrained linkages [**6**].

The authors have shown that not only does the construction process apply to single Bennett linkage, but also it can be extended to the grid of Bennett linkages. A number of physical models were built to demonstrate the concept. All of them worked well. Although the models simply use members with square cross-sections, it is not necessary so in

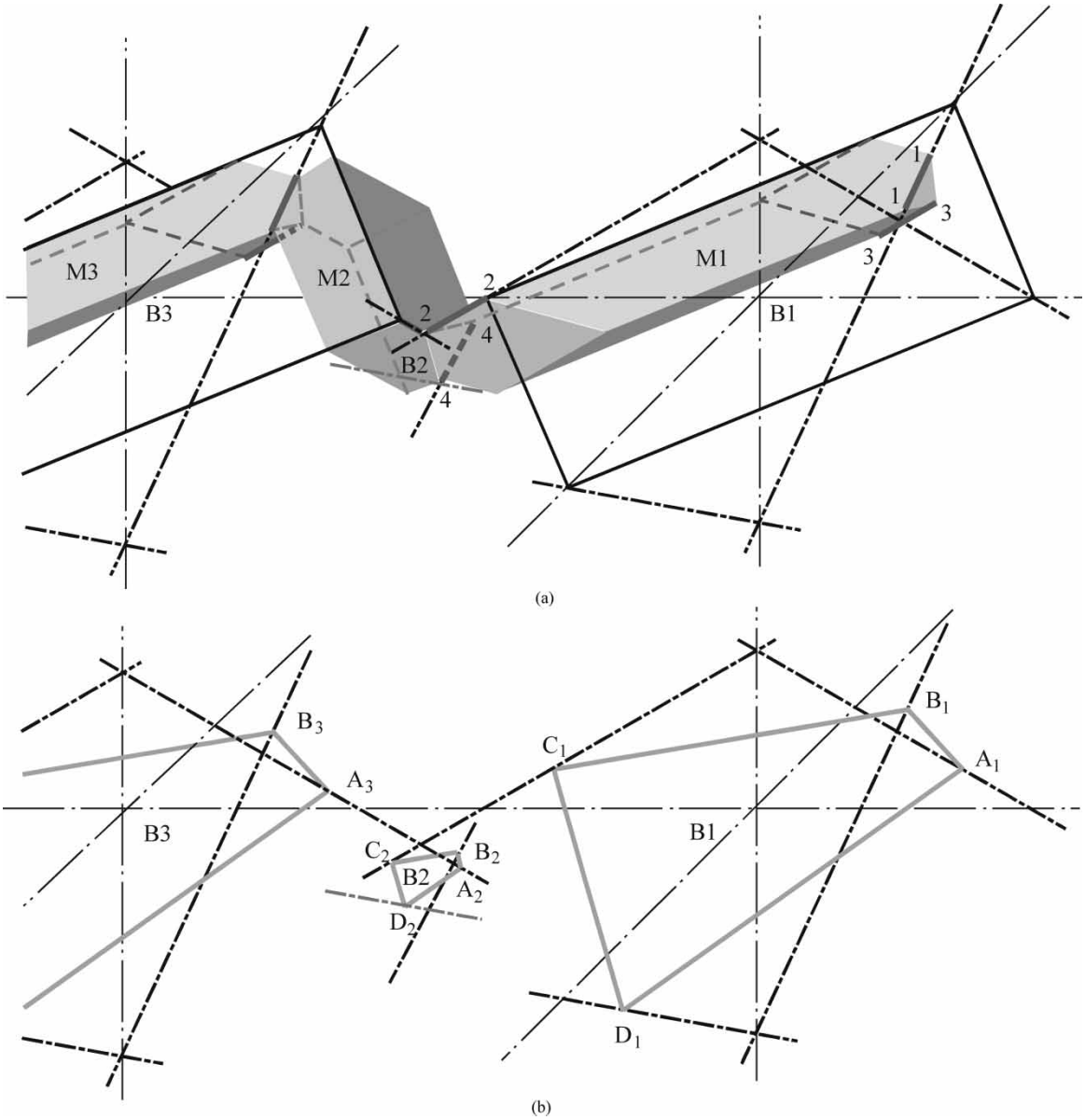

Fig. 10 (a) The schematic diagram of a grid consisting of Bennett linkages in their alternative forms. Only one member is shown in each Bennett linkage. (b) The corresponding grid of original Bennett linkages

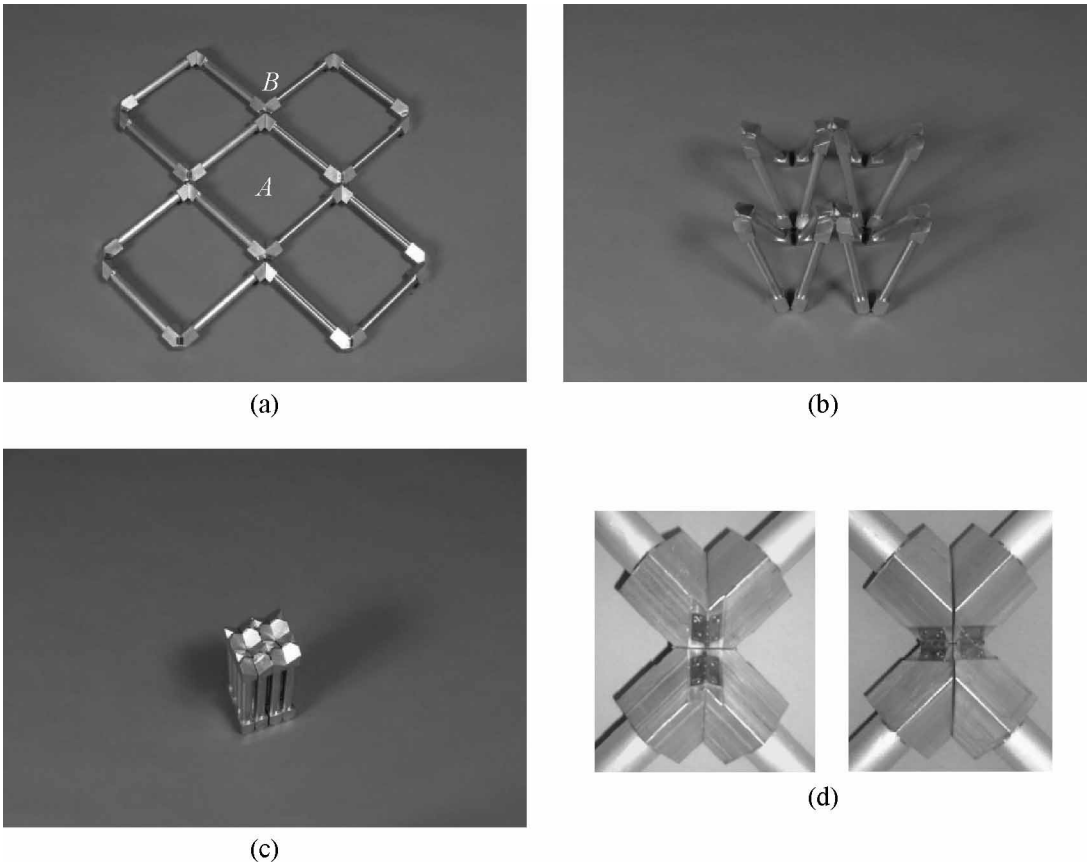

Fig. 11 A model of assembly of the Bennett linkages in the alternative form. (a) to (c) Folding sequence of a model in the alternative form and (d) Front and rear views of the joints

large-scale applications in which weight is a main concern. More efficient structural forms, e.g. trusses, hollow square tubes, and so on, can be used to replace solid members as long as the hinges are positioned at right locations.

It should be pointed out that when the models are fully folded, all the members are mathematically colinear. Hence, there exists a configuration-dependent state of self-stress, e.g. two of the members can have the same tensile force, whereas the other two have a compression force of equal magnitude. Associated with it would be an increment of 1 in the kinematic indeterminacy or a kinematic bifurcation in the motion path of the linkage [**7**–**9**]. However, this does not cause any problem in reality due to the fact that the members would have to penetrate each other in order to reach the bifurcated position, which is physically impossible. This also explains why there is only one possible motion for the assembly.

Another special case is that when the twist α becomes $\pi/2$, the movement of the Bennett linkage is separated into two stages. In stage 1, it opens up about two opposite hinges, which remain parallel until it folds up completely, and in stage 2, it deploys about the other two hinges. At this particular twist, there is no difference between the Bennett linkage in its original form and its alternative form.

This type of frame is ideal for aerospace applications to provide support structures for flexible solar blanket or reflective surfaces. Potential users of the structures need also to be aware that the motion of two opposite members in an assembly does not move in parallel, so the flexible surfaces cannot be simply rolled around them. A solution to this problem is to fold up the flexible surfaces using an origami folding pattern, which matches the motion of the members. This is found to be possible, but the detailed discussion would prolong the article. The interested readers could contact the authors for further information.

ACKNOWLEDGEMENTS

The authors would like to express their gratitude to the workshop of the Department of Engineering Science, Oxford University for their craftsmanship in making the wonderful models. This work is

supported by the Engineering and Physics Research Council in the form of a research grant (GR/M61207). Y. Chen would like to thank the University of Oxford for a graduate student scholarship. Z. You is grateful to the Royal Academy of Engineering from which he received a Global Research Award that enabled him to complete this paper.

REFERENCES

1 **Chen, Y.** and **You, Z.** Square deployable frames for space applications. Part I: theory. *Proc. IMechE, Part G: J. Aerospace Engineering*, 2006, **220**(G4), 347–354.
2 **Crawford, R. F., Hedgepeth, J. M.,** and **Preiswerk, P. R.** *Spoked wheels to deploy large surfaces in space: weight estimates for solar arrays*. NASA-CR-2347, 1973.
3 **Pellegrino, S., Green, C., Guest, S. D.,** and **Watt, A.** SAR advanced deployable structure. Technical Report, Department of Engineering, University of Cambridge, 2000.
4 **Chen, Y.** and **You, Z.** Network of Bennett linkages as deployable structures. AIAA Space 2001 Conference and Exposition, Albuquerque, USA, 28–30 August 2001, AIAA 2001-4661.
5 **Chen, Y.,** and **You, Z.** Mobile assemblies based on the Bennett linkage. *Proc. R. Soc. A*, 2005, **461**, 1229–1245.
6 **Chen, Y., You, Z.** and **Tarnai, T.** Threefold-symmetric Bricard linkages for deployable structures. *Int. J. Solids Struct.*, 2005, **42**, 2287–2301.
7 **Calladine, C. R.** Buckminster Fuller's 'tensegrity' structures and Clerk Maxwell's rules for the construction of stiff frames. *Int. J. Solids Struct.*, 1978, **14**, 161–172.
8 **Calladine, C. R.** and **Pellegrino, S.** First-order infinitesimal mechanisms. *Int. J. Solids Struct.*, 1991, **27**, 505–515.
9 **Phillips, J.** *Freedom of machinery*, 1990, vol. 2 (Cambridge University Press, Cambridge, UK).